Forced Convection in a Polymeric Powders

Jeffery L. Norrell
Graduate Research Asst.

Kristin L. Wood
Associate Professor

Richard H. Crawford
Associate Professor

Mechanical Engineering Department
The University of Texas at Austin

Theodore L. Bergman
Professor

Mechanical Engineering Department
The University of Connecticut

Abstract

In a Selective Laser Sintering (SLS) powder bed, thermal transfer occurs through multiple modes. Forced convection through the powder, or downdraft, has recently been implemented in SLS machines in an effort to enhance thermal transfer within the powder bed. In this paper, forced convection is analytically shown to be a significant thermal transfer mode for low porosities, such as seen in SLS powder beds. A polymeric powder bed subjected to downdraft is investigated with the goal of quantitatively determining thermal behavior. A numerical model describing heat transfer within a powder is presented. The design and construction of an experimental apparatus to measure the temperature profiles within a powder subjected to forced convection is described. Using the information gained in these experiments, it may be possible to better control the thermal environment of SLS powder beds, reducing growth and internal stress build-up.

Nomenclature

c_{pf}	= specific heat, fluid (J/kg K)
g	= gravitational acceleration (m/s^2)
K	= permeability (m^2)
k_{eff}	= effective thermal conductivity of powder (W/mK)
k_f	= thermal conductivity of fluid (W/mK)
p	= pressure (Pa)
T	= absolute temperature (K)
T_c	= cold temperature (K)
t	= time (seconds)
u, v	= x and y velocity components (m/s)
u_D, v_D	= Darcian x and y velocity components (m/s)
x, y	= horizontal and vertical coordinate (m)
β	= coefficient of thermal expansion (K^{-1})
ϕ	= volume-averaged porosity
μ_{eff}	= effective (in-powder) fluid viscosity (Ns/m^2)
μ	= fluid viscosity (Ns/m^2)
ρ	= density of fluid phase (kg/m^3)

Introduction

Selective Laser Sintering (SLS) is one of the many Rapid Prototyping methods currently available today. In SLS, a part is layer-wise formed by laser-melting a loose powder. Such a process is inherently dominated by thermal processes, both between the laser and powder and within the powder bed.

Typical gas-saturated, polymeric powder beds complicate control of the thermal environment by being excellent thermal insulators due to the low thermal conductivity of both the polymer and saturating gas. Thermal control of the powder bed is critical to prevent unwanted effects such as part growth and warping. Many methods, such as radiative surface heaters and resistive wall heaters, have been attempted to achieve fine, rapid control over the thermal state of a powder bed.

Another method, shown to have at least a qualitative effect on part quality, is forced convection through a powder. In current commercial SLS systems, a pressure drop is created below the powder bed to induce gas flow. Radiative heaters are used to heat the upper surface of the powder bed. In theory, gas then flows through this upper portion of the powder bed where the gas is heated. The gas then flows through the remaining portion of the powder bed, carrying thermal energy to the remainder of the powder.

The goal of this work is to create a numerical model describing forced convection within a powder. Once such a model is obtained, experiments will be performed for model validation.

Numerical Model

The two-dimensional arrangements depicted in Figure 1, display the computational domains considered. Figure 1(a) is the domain for a pure conduction simulation, whereas Figure 1(b) is the domain for a forced convection simulation, both with and without buoyant forces.

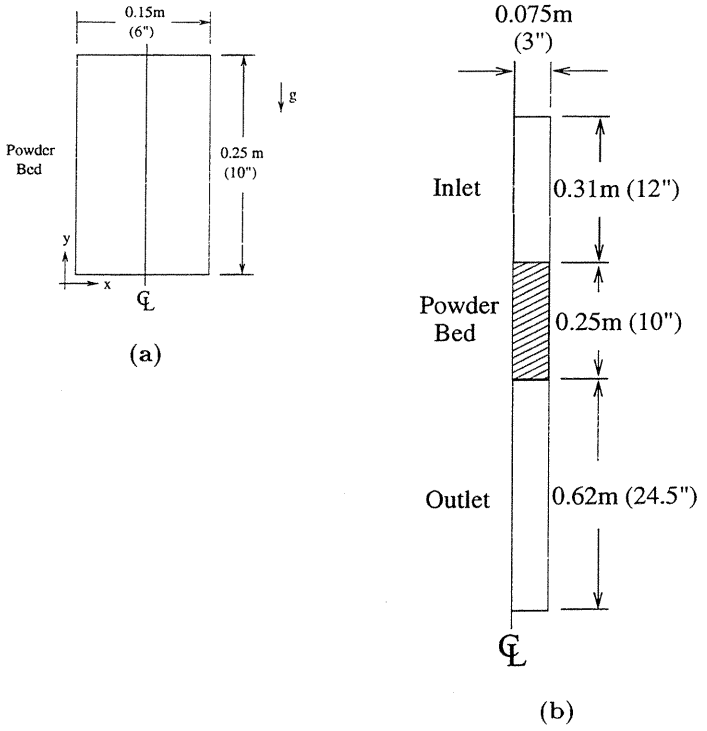

Figure 1: Computational domains.

In this simulation, heated air, assumed to be slug flow, enters the top of the inlet. The heated air then passes through the powder bed, leaving the system via the outlet. An analytical model is created to describe heat transfer in this system. The governing equations for the pure fluid and the

saturated porous medium are given separately. In writing the following equations, it is assumed that fluid flow is laminar, steady, incompressible, and two-dimensional.

For the pure fluid region, the two-dimensional, steady state Navier-Stokes equations are used [4]. Conservation of mass is given by,

$$\frac{\partial u}{\partial x}+\frac{\partial v}{\partial y}=0. \tag{1}$$

Conservation of momentum within the pure fluid is described by,

$$\rho\left(u\frac{\partial u}{\partial x}+v\frac{\partial u}{\partial y}\right)=-\frac{\partial p}{\partial x}+\frac{\partial}{\partial x}\left(\mu_f\frac{\partial u}{\partial x}\right)+\frac{\partial}{\partial y}\left(\mu_f\frac{\partial u}{\partial y}\right), \tag{2}$$

and

$$\rho\left(u\frac{\partial u}{\partial x}+v\frac{\partial u}{\partial y}\right)=-\frac{\partial p}{\partial y}+\frac{\partial}{\partial x}\left(\mu_f\frac{\partial v}{\partial x}\right)+\frac{\partial}{\partial y}\left(\mu_f\frac{\partial v}{\partial y}\right)+\rho g\beta\left(T-T_c\right). \tag{3}$$

Conservation of energy is expressed as,

$$\rho c_{pf}\left(u\frac{\partial T}{\partial x}+v\frac{\partial T}{\partial y}\right)=\frac{\partial}{\partial x}\left(k_f\frac{\partial T}{\partial x}\right)+\frac{\partial}{\partial y}\left(k_f\frac{\partial T}{\partial y}\right). \tag{4}$$

It is important to note that the thermophysical properties of the pure fluid are assumed constant. The exception is during buoyant simulations, where a Boussinesq approximation of fluid density, in which density varies with temperature, is used.

For a fluid-saturated porous medium, the volumetrically-averaged laminar, inviscid, isothermal fluid flow is approximately described by the Darcy equation [1],

$$\frac{\Delta p}{\Delta y}=\frac{\mu_f}{K}v \tag{5}$$

To account for non-isothermal fluid flow, a Brinkman-Forchheimer extended version of the Darcy model is used [2,5]. Within the saturated powder Darcian, or volumetrically-averaged, velocities are used. Conservation of mass within the saturated powder is then given by,

$$\frac{\partial u_D}{\partial x}+\frac{\partial v_D}{\partial y}=0. \tag{6}$$

Conservation of momentum is given by,

$$0=-\frac{\partial p}{\partial x}+\frac{\partial}{\partial x}\left(\mu_{eff}\frac{\partial u_D}{\partial x}\right)+\frac{\partial}{\partial y}\left(\mu_{eff}\frac{\partial u_D}{\partial y}\right)-\left(\frac{\mu_f}{K}+\frac{\rho C}{\sqrt{K}}|\vec{u}_D|\right)u_D, \tag{7}$$

and,

$$0=-\frac{\partial p}{\partial y}+\frac{\partial}{\partial x}\left(\mu_{eff}\frac{\partial v_D}{\partial x}\right)+\frac{\partial}{\partial y}\left(\mu_{eff}\frac{\partial v_D}{\partial y}\right)+\rho g\beta\left(T-T_c\right)-\left(\frac{\mu_f}{K}+\frac{\rho C}{\sqrt{K}}|\vec{u}_D|\right)v_D. \tag{8}$$

Equations (7) and (8) include the Brinkman extension (second and third terms) and the Forchheimer extension (the last term) to account for viscous and inertial effects, respectively.

Conservation of energy is described by,

$$\rho c_{pf}\left(u_D\frac{\partial T}{\partial x}+v_D\frac{\partial T}{\partial y}\right)=\frac{\partial}{\partial x}\left(k_{eff}\frac{\partial T}{\partial x}\right)+\frac{\partial}{\partial y}\left(k_{eff}\frac{\partial T}{\partial y}\right) \tag{9}$$

All thermophysical properties are again assumed constant, except for a Boussinesq density approximation in buoyant simulations. In Equations (7) and (8), $\mu_{eff}=\mu_f$, which has been

previously seen to agree well with experimental data [8]. It is important to note that Equations (6) through (8) neglect any radiation heat transfer between the fluid and powder or within the powder itself.

The term k_{eff} in Equation (9) is the effective thermal conductivity of the fluid-saturated powder bed. Though many expressions are available for k_{eff} [6,7,9,10], a simple weighted average,

$$k_{eff} = \phi k_f + (1 - \phi) k_s, \tag{10}$$

is used. The C term in equations (7) and (8) is the inertia coefficient given as [3],

$$C = \frac{1.75}{\sqrt{175}} \phi^{-3/2}. \tag{11}$$

The above analytical model is numerically solved for the two-dimensional, steady state temperature distribution within both the fluid and fluid-saturated powder using the commercial finite-element code FIDAP (version 7.5 from Fluid Dynamics International).

Experiments

Test Materials

In order to experimentally verify the numerical model presented above, an experimental apparatus, shown in Figure 2(a), was constructed. The working fluid for these experiments is air, while the powder bed consists of polycarbonate with a nominal particle diameter of 150 μm and an average poured porosity of 0.5. Regarding permeability, there are no general equations relating permeability as a function of porosity [5]. A number of empirical models exist, but all have restrictions in their application. If we consider equation (5), we see that for an isothermal system with known geometry, we can control flow rate, measure the pressure drop across the powder, and calculate a permeability. For a 0.025 m (1") thick, 0.25 m (1") diameter powder sample, subjected to a flow of 0.31 m/s (20 SCFH) to 0.62 m/s (40 SCFH), a pressure drop of approximately 1 kPa is measured. From Equation (5), we then determine that the powder permeability is approximately $1.5\text{x}10^{-10}$ m^2.

Experimental Instrumentation

Dimensions of the major sections of the experimental system are as shown in Figure 1(b). In the experiment, compressed air passes over PID-controlled baffle heaters and then enters a plenum. Once through the plenum, the heated air passes through the inlet, through the powder bed, and leaves the system via the outlet.

The baffle heaters are housed in a 0.10 m x 0.10 m (4" x 4") uninsulated plywood box. The baffles are separated vertically by 0.00635 m (1/4"). The baffle box opens into a 0.15 m x 0.15 m x 0.025 m (6" x 6" x 1") plywood plenum, which sits atop the inlet. The inlet section is constructed of 0.15 m (6") ID polyvinyl chloride (PVC) pipe. Mounted on the outside of the inlet section is a 100 W PID-controlled resistive heater covered with fiberglass insulation, used to maintain a quasi-isothermal boundary for the inlet. The inlet is mounted on top of the powder bed, which is housed in 0.15 m (6") ID steel pipe. The powder bed is surrounded by a fluid circulation jacket, also used to maintain an isothermal boundary. The powder bed sits atop a fine wire mesh, allowing airflow through the powder. Pressure drop across the mesh alone was measured to be less than 1 Pa. Below the powder bed sits the outlet, constructed of 0.15 m (6") ID PVC pipe. Given the relatively low temperatures in the outlet section and the high thermal mass of the PVC pipe, fiberglass insulation alone

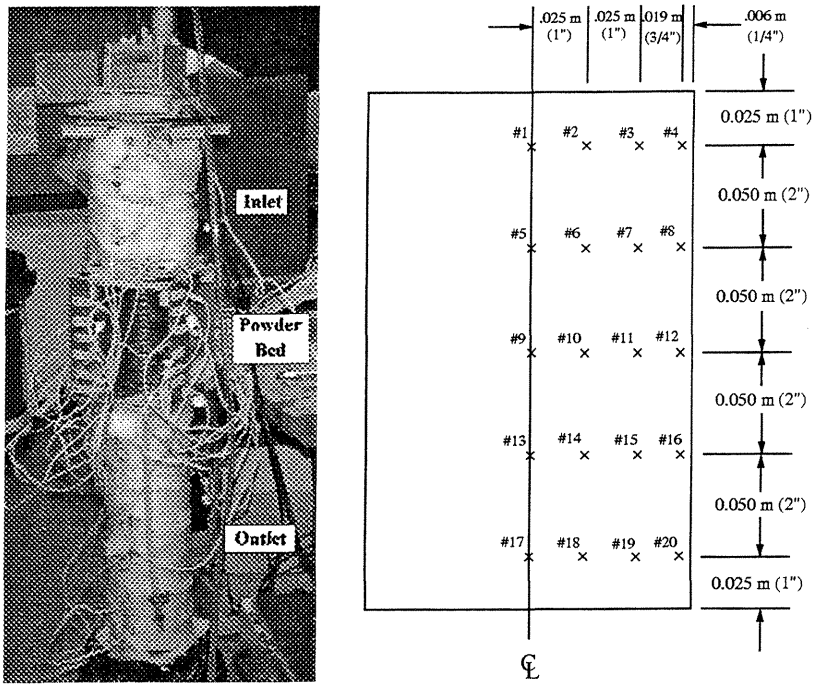

(a) Apparatus. (b) Thermocouple numbering.

Figure 2: Experimental system.

sufficiently maintains an isothermal boundary condition. An optional fan can be placed beneath the outlet to induce a pressure drop below the powder bed, further inciting airflow through the powder.

Throughout the experimental device, 125 μm (5 mil), type K, PTFE-coated thermocouples are used to gather temperature data. A thermocouple is placed in the powder bed at each location marked with an "x" shown in Figure 2(b). Thermocouples also record air temperature in the inlet and outlet. All thermocouple data are collected and recorded with a Keithley 500A computer-controlled data acquisition unit.

The experimental system has several user-controlled inputs. Incoming compressed air can be heated from 25 ° C to 150 ° C, over a flow range of 0.017 m/s (40 SCFH) to 0.034 m/s (80 SCFH) in the inlet. The inlet wall can be heated from 25 ° C to 100 ° C. The fluid circulation jacket can be maintained over a range of temperatures from approximately 30 ° C to 100 ° C.

Experimental Procedure

In preparing for the experiment, the powder bed, wire mesh, and outlet, all initially at room temperature, are assembled together. Next, 0.025 m (1") of room temperature powder is poured inside. The steel powder bed wall is then repeatedly tapped, allowing the powder to settle. This procedure of pouring in powder then tapping is repeated, until the desired powder depth is achieved. The powder surface is then smoothed, and the remaining sections of the experimental device are assembled.

Once initial assembly is completed, data acquisition is started. Airflow into the system and fluid flow into the fluid circulation jacket are then begun. The heated baffles and inlet wall heater

are next ramped to temperature over a period of 30 minutes.

The system is left to run until thermal steady state is achieved. Typically, a run lasts from 8 to 15 hours. At this time, the recorded temperature data are downloaded and checked to verify that steady state has been achieved.

Results

Two separate tests were run for comparison with the numerical model. For these two tests, the temperature set point for the incoming air was kept constant at 100 ° C, while the flow rate was varied. For each test, three numerical simulations were performed.

The first test was run with an airflow of 0.017 m/s (40 SCFH). Measured temperatures as a function of time are shown in Figure 3. Data curve labels indicate the thermocouple number, with Figure 2(b) indicating the in-bed position of the given thermocouple.

For comparison, numerical simulations were also performed. Temperatures measured during the 40 SCFH experiment were used as boundary conditions in the simulations. Figure 4(a) shows the conduction heat transfer simulation for the powder bed. Figures 4(b) and 4(c),covering one-half of the experimental domain, show simulations that include both forced convection and conduction heat transfer. Figure 4(c), a buoyant simulation, also adds the Boussinesq air density approximation. The Δ T between isotherms in Figure 4 is 4° C.

The second experiment was run with an airflow of 0.025 m/s (60 SCFH). Figure 5 shows the measured temperatures as a function of time.

Figure 6 shows the numerical simulations run for the 60 SCFH experiment, where again Figure 6(a) is the conduction simulation, Figure 6(b) is the forced convection solution without buoyant forces, and Figure 6(c) is the convection solution with buoyant forces. As above, the Δ T between isotherms is 4 ° C.

Discussion

In terms of numerical results, by comparing Figure 4(a) to 4(b) and Figure 6(a) to 6(b) we see that, *numerically*, forced convection can have a significant impact on heat transfer within a polymeric powder bed. Keep in mind that Figures 4(a) and 6(a) represent the entire powder bed and Figures 4(b) and 6(b) represent *half* of the physical domain. Comparison is then made by considering isotherms of the same value in Figures 4(a), 4(b), and 4(c), and their location within the powder bed region. From this comparison, we can see that, in effect, forced convection works to transport thermal energy further into the powder.

By considering Figure 4(b) versus 4(c) and Figure 6(b) versus 6(c), we can also see that natural convection, i.e. buoyancy-induced flow, can have a significant effect at these low flow rates. Also, from comparing Figure 4(b) to Figure 6(b), we see that increasing flow velocity through a powder increases thermal transfer into the deeper parts of the bed, as expected.

In terms of the experimental results, we can see from both Figures 3 and 5 that achieving steady state, the point where dT/dt approaches zero and the temperature versus time curves begin to flatten out, can take a significant amount of time, over 7 hours. Air and polycarbonate, both relatively good thermal insulators alone, make an even better thermal insulator in the form of an air-saturated powder bed.

If we compare the experimental data to the forced convection simulations, both with and without buoyancy, we begin to see a discrepancy. The experimentally-measured temperatures are signifi-

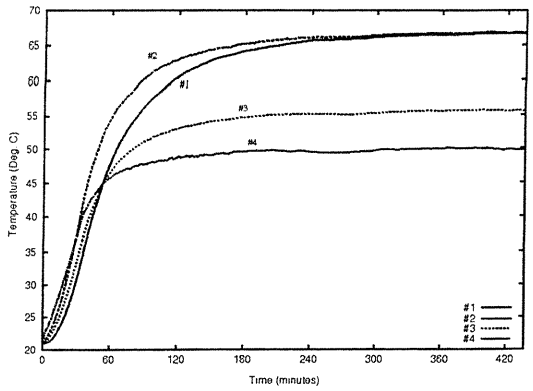

(a)

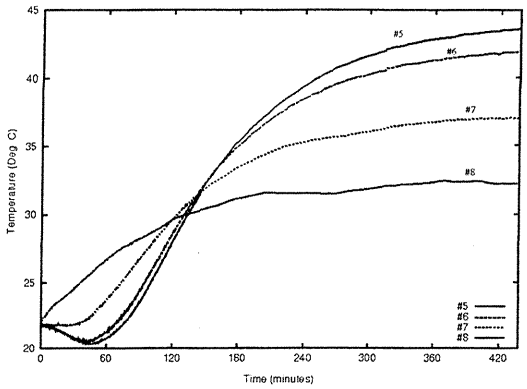

(b)

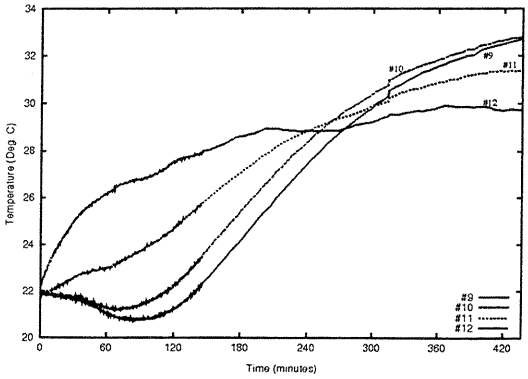

(c)

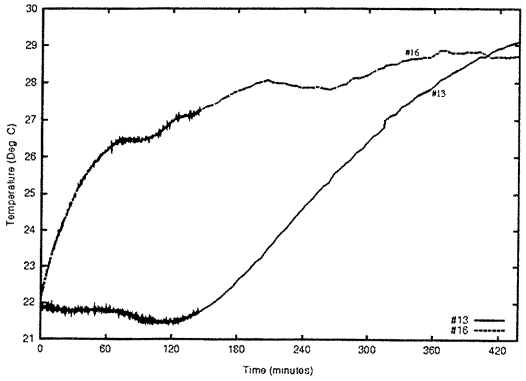

(d)

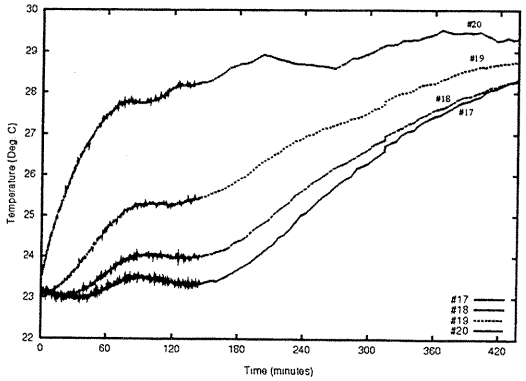

(e)

Figure 3: Experimental data for 40 SCFH simulation.

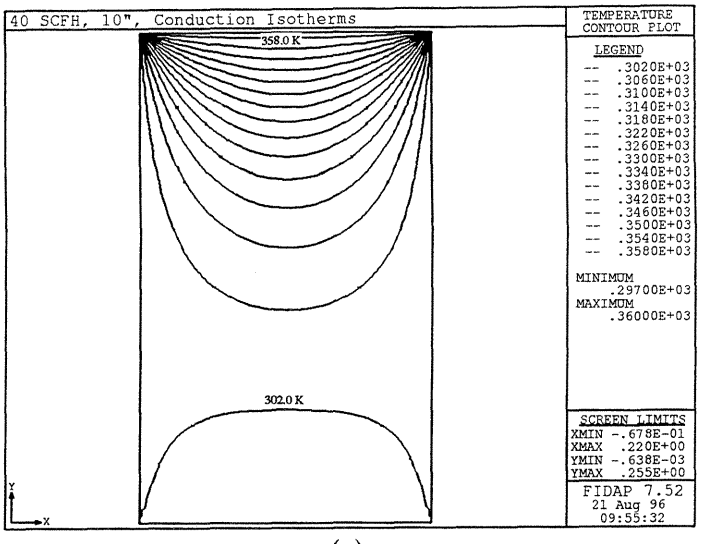

(a)

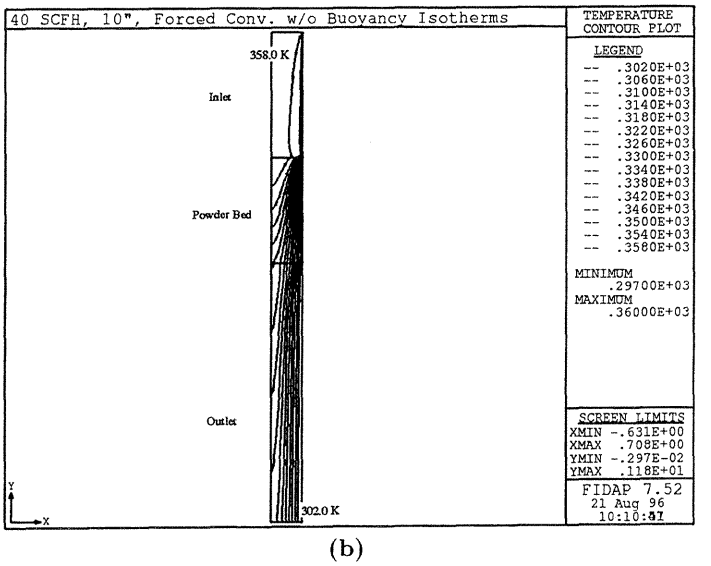

(b)

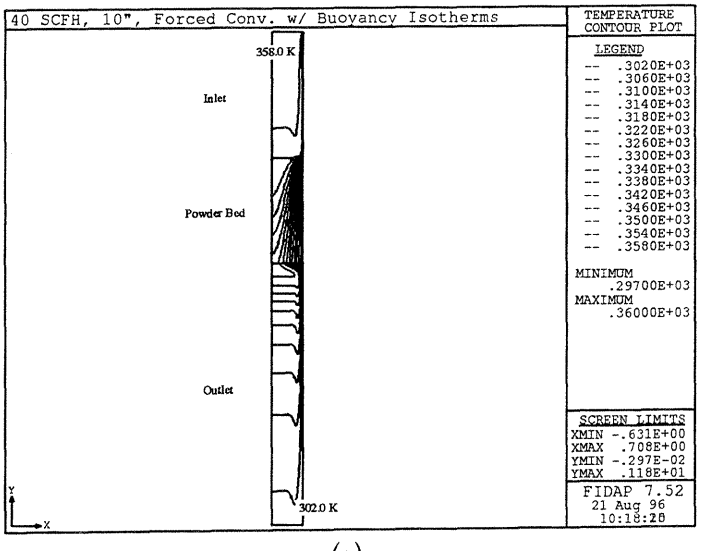

(c)

Figure 4: Isotherms for 40 SCFH simulation.

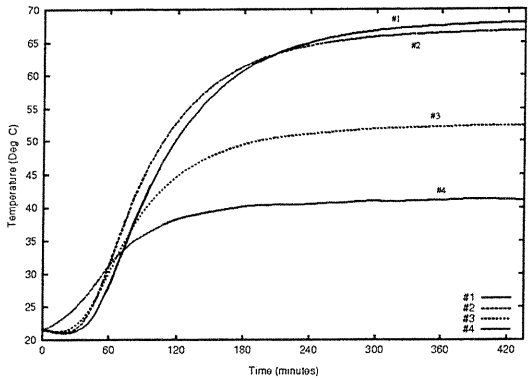

(a)

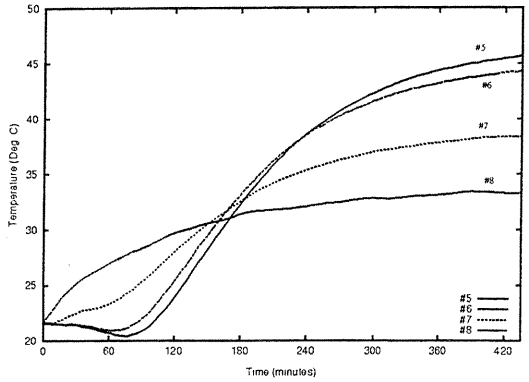

(b)

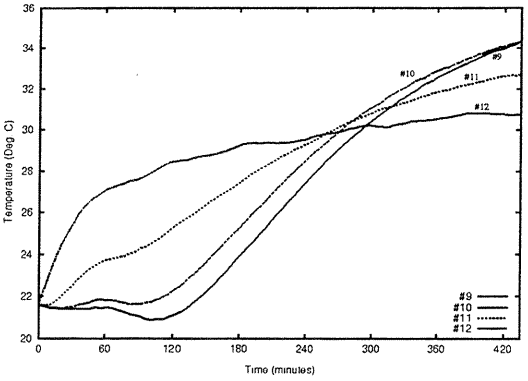

(c)

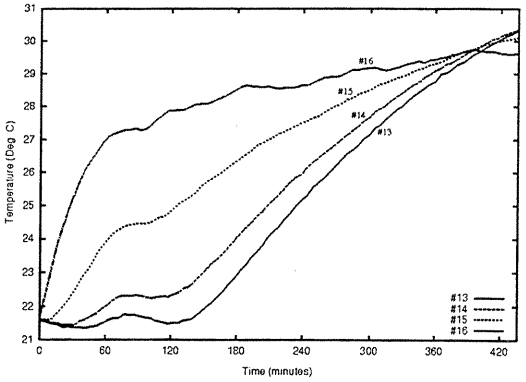

(d)

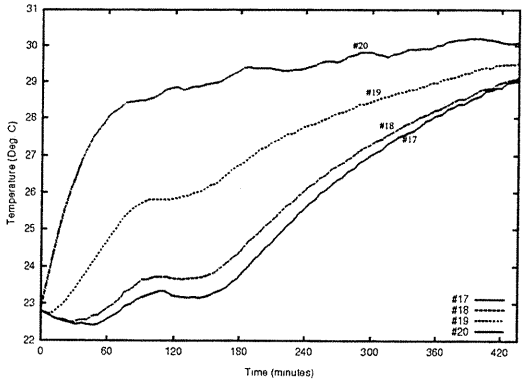

(e)

Figure 5: Experimental data for 60 SCFH simulation.

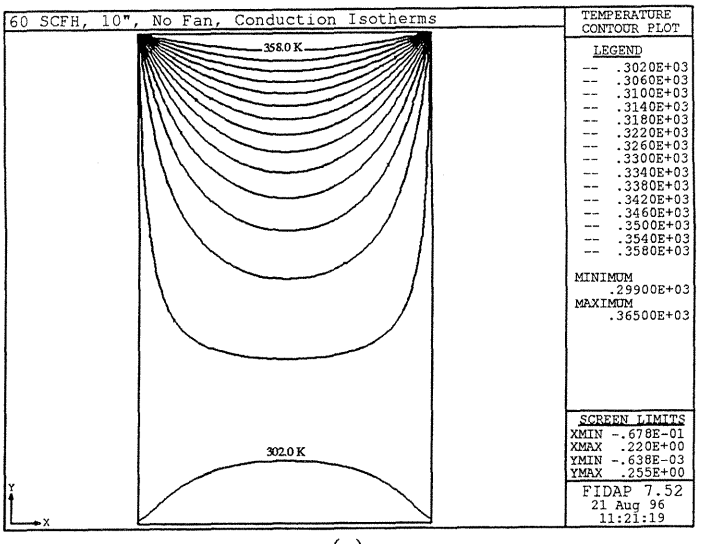

(a)

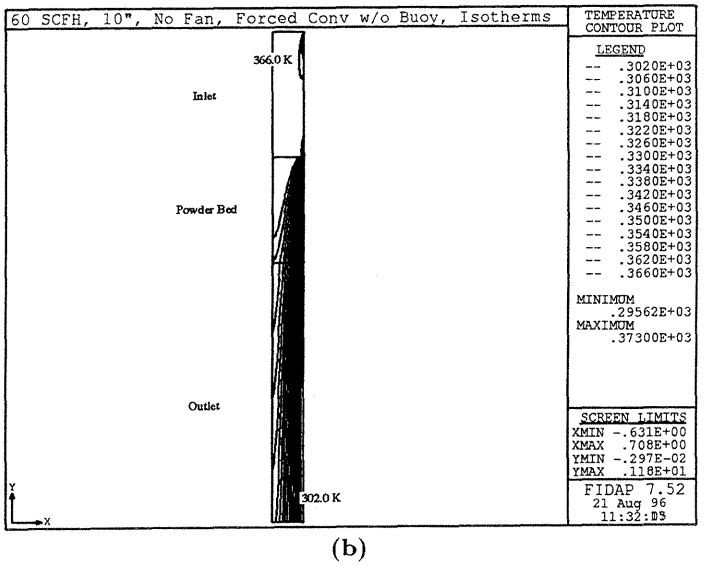

(b)

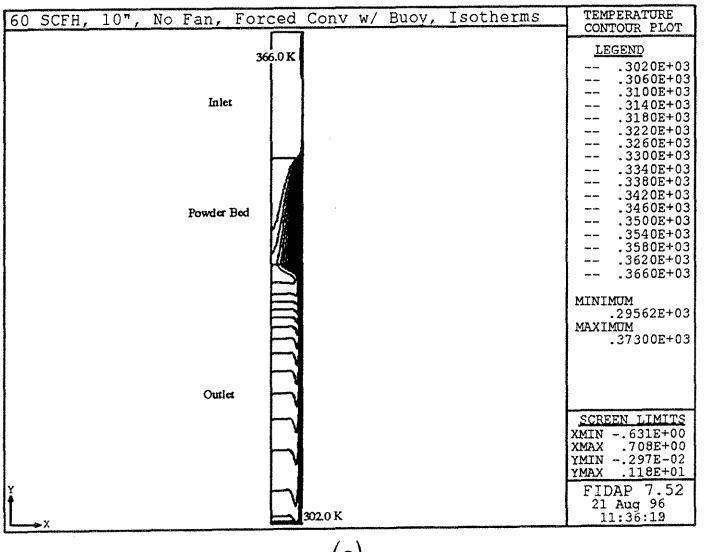

(c)

Figure 6: Isotherms for 60 SCFH simulation.

cantly lower than those predicted in the forced convection simulations. However, if the measured temperatures are compared to the *conduction* simulation, we see that there is excellent agreement.

As in any research, a discrepancy between model and experiment implies a flaw in the model. In this instance, it is believed that the numerical model does not adequately reflect the air leaks present in the experimental apparatus. In essence, the resistance to flow imposed by the low permeability powder forces the air out of mating surfaces in the experiment. At present, these leaks prevent any *experimentally* driven conclusions about forced convection heat transfer within a polymeric powder. However, we can easily see from Figures 3 and 5 that conduction heat transfer within a polycarbonate powder bed can take a significant amount of time to have any effect on the bed interior.

Conclusions and Future Work

Numerically, forced convection heat transfer is seen to have a significant effect on steady state temperatures within an air-saturated polymeric powder bed. It is also numerically shown that, at sufficiently low flow rates, natural convection, or buoyancy-induced flow, must be accounted for in simulations.

Experimentally, it is seen that the low permeability of fine powders, which are typically used in SLS, can have a drastic effect on attempts at generating flow through the powder. Much care must be taken to ensure that fluid is, in actuality, flowing through the powder.

Once true airflow through a powder is achieved and verified against the numerical model, fractional experiments will be performed. Control variables will be the initial air temperature, powder bed wall temperature, and airflow rate. In addition, a polymeric sintering model based on solid mechanics will be formulated and added to the numerical heat transfer. In conjunction with the model development, experiments will be undertaken wherein a heated object is embedded in the powder bed, reflecting the latent heat in a recently formed SLS part. In this way, sintering of the polymer under influence of forced convection can be studied. Information gained from these studies can then be used to better control the thermal state of a polymeric powder bed. More precise and rapid control may then help alleviate such nagging problems as growth and part warpage.

Bibliography

1. Bear, J., 1972, *Dynamics of Fluids in Porous Media*, American Elsevier, New York.

2. Beckermann, C., Ramadhyani, S., and Viskanta, R., 1987, "Natural Convection Flow and Heat Transfer Between a Fluid Layer and a Porous Layer Inside a Rectangular Enclosure," *J. Heat Trans.*, Vol. 109, pp. 363-370.

3. Ergun, S., 1952, "Fluid Flow Through Packed Columns," *Chem. Eng. Prog.*, Vol. 48, pp. 89-94.

4. Incropera, F.P., and De Witt, D.P., 1990, *Fundamentals of Heat and Mass Transfer*, Third ed., John Wiley and Sons, New York, NY.

5. Kaviany, M., 1991, *Principles of Heat Transfer in Porous Media*, Springer-Verlag, New York.

6. Krupiczka, R., 1967, "Analysis of Thermal Conductivity in Granular Materials," *J. Int. Chem. Eng.*, Vol. 7, No. 1, pp. 122-144.

7. Kubie, J., 1987, "Steady-State Conduction in Stagnant Beds of Solid Particles," *Int. J. Heat and Mass Trans.*, Vol. 30, No. 5, pp. 937-947.

8. Neale, G., and Nader, W., 1974, "Practical Significance of Brinkman's Extension of Darcy's Law: Coupled Parallel Flows Within a Channel and a Bounding Porous Medium," *Canadian J. Chem. Eng.*, Vol. 52, pp. 475-478.

9. Xue, S., and Barlow, J.W., 1991, "Models for the Prediction of the Thermal Conductivities of Powders," *Proceedings, Solid Freeform Fabrication Symposium*, H. Marcus, et al., ed., Austin, TX, pp. 62-69.

10. Yagi, S., and Kunii, D., 1957, "Studies on Effective Thermal Conductivities in Packed Beds," *J. AICHE*, Vol. 3, No. 3, pp. 373-381.